J. Physiol. (1965), **180**, *pp.* 607–635
With 16 *text-figures*
Printed in Great Britain

ELECTRICAL BEHAVIOUR OF THE MOTONEURONE MEMBRANE DURING INTRACELLULARLY APPLIED CURRENT STEPS

BY M. ITO* AND T. OSHIMA†

From the Department of Physiology, John Curtin School of Medical Research, The Australian National University, Canberra, Australia

(*Received* 13 *January* 1965)

The electrical properties of the motoneurone membrane have so far been investigated by many workers by the use of intracellular application of current steps (Coombs, Eccles & Fatt, 1955*a*; Araki & Otani, 1955; Frank & Fuortes, 1956; Coombs, Curtis & Eccles, 1959). The changes in transmembrane potential thus produced have been interpreted on the basis of the conventional capacitance-resistance model of the membrane. However, Araki, Ito & Oshima (1962) have recently noticed a rather peculiar behaviour of the motoneurone membrane of the cat; on application of current steps, the potential change reaches a maximum at about 15 msec after the onset of current and thereafter declines gradually to a steady level, stabilizing within about 100 msec. After the current ceases, the potential undershoots the original level and recovers thereto with a time course similar to the decline of the overshoot. This paper gives an account of a systematic investigation of these over- and undershoots, and in the discussion it will be found necessary to develop new concepts with respect to the electrical properties of the motoneurone membrane.

METHODS

Fourteen cats were used under anaesthesia induced by pentobarbitone sodium. The spinal cord was cut at the L1 or L2 level. The general plan of the dissection and experimental arrangement was similar to that described by Araki, Ito & Oscarsson (1961). Intracellular application of current steps and recording of the potential changes thereby produced across a motoneurone membrane were carried out with double or single micro-electrodes.

Double micro-electrodes were of the same type as those used by Coombs *et al.* (1955*a*) and filled with solution containing 3 M-KCl or in a few cases 2 M-K citrate by the mechanical method of Ito, Kostyuk & Oshima (1962). Electrodes with an electrical resistance of 7–10 MΩ for each barrel and with an interbarrel coupling resistance of less than 100 kΩ

* Present address: Department of Physiology, Faculty of Medicine, University of Tokyo, Tokyo, Japan.

† Present address: Department of Neurophysiology, Institute of Brain Research, Faculty of Medicine, University of Tokyo, Tokyo, Japan.

were selected (cf. Coombs *et al.* 1955*a*). One barrel of an electrode was used for recording in connexion with an input cathode follower. Another barrel was connected in series to a 10 MΩ and a 100 MΩ resistor, the latter being further connected to a current generator. The current strength usually was monitored by a differential d.c. recording of the voltage drop across the 10 MΩ resistor. In some experiments where relatively large currents were employed, their intensity was measured by recording from a 2 kΩ resistor inserted between the cat body and the earth (see Fig. 10). Artifact potential due to current flow through the interbarrel coupling capacitance (Coombs *et al.* 1955*a*) was reduced by applying the current steps, their phase being reversed, to the recording barrel through a small capacitor (Eccles, Eccles & Ito, 1964*a*). The artifact still remaining was due not only to the interbarrel coupling capacitance but also to the common resistance, and it was recorded in the extracellular position after withdrawal of the microelectrode (see Fig. 1). The net change across the cell membrane was derived by subtracting the artifact potential from the intracellularly recorded potential (Coombs *et al.* 1955*a*). Owing to the small artifact, the double microelectrodes were preferred for obtaining the potential changes during a wide range of current intensities.

Single micro-electrodes were filled with 3 M-KCl solution and those with electrical resistance of 7–10 MΩ were selected. An electrode was used in connexion with the input circuit designed by Ito (1960) and further with a 10 MΩ and a 100 MΩ resistor in series, the latter being connected to a current generator. Changes in the membrane potential of impaled cells were recorded during current passage by compensating for the voltage developed across the electrode resistance at the stage of the main d.c. amplifier (Ito, 1957). The current intensity was monitored by a differential d.c. recording from the 10 MΩ resistor. A disadvantage with the single-electrode technique is the non-linear and time-dependent change of the electrode resistance which occurs during passage of currents and so obscures the net change in the membrane (Frank & Fuortes, 1956). This electrode polarization is, however, small with current steps of less than 3×10^{-9} A (Ito, 1957). Therefore, analysis in the present work was made only on the potential changes induced by current of less than 3×10^{-9} A. Under such conditions there was a small electrode polarization that could be examined in isolation in the extracellular position and in addition either in a solution of 0·15 M-KCl or 0·15 M-K glutamate which were kept in small beakers mounted on the back muscles of the cat. The K glutamate solution may approximate to the intracellular fluid which, in contrast to the sodium-rich extracellular medium, involves potassium ions and large organic anions in a high concentration. Usually there was virtually no difference between electrode polarizations in the extracellular and potassium solutions. The net change in the membrane was derived approximately by correcting for the electrode polarization from the intracellularly recorded potential change (see Figs. 6 and 7). The amplitude of the potential changes induced across the motoneurone membrane by currents of less than 3×10^{-9} A was only several millivolts; hence it was necessary to minimize the synaptic noise of the motoneurones (Brock, Coombs & Eccles, 1952) by administering intravenously 30–40 mg pentobarbitone sodium/kg of the cat body weight every 2 hr or so. Artificial respiration was employed if respiration was too depressed. Exact comparison was not made, but it was a general impression that such a deep anaesthesia as this did not influence significantly the membrane properties concerned in the present work.

The potential changes recorded from the motoneurone membrane were amplified by two d.c. amplifiers with different gains (see Figs. 4 and 11). Records were taken by 5 to 20 repeated sweeps at a rate of 0·5–2 c/s, the sweep rate being varied according to the duration of current steps. Care was taken to maintain the temperature of the cat body and the paraffin pool immersing the spinal cord at 37–38° C.

RESULTS

The magnitude of over- and undershoots

In the experiments shown in Fig. 1, current steps of about 250 msec duration and of four different amplitudes within the range of $0–2{\cdot}2 \times 10^{-8}$ A were passed across a motoneurone membrane through one barrel of a double micro-electrode, the potential change thereby induced being recorded through the other barrel. In this recording, as shown in the bottom traces of each record of Fig. 1, there were only small artifact potentials due to interbarrel coupling resistance of about 50 kΩ. On applying and withdrawing the current in either depolarizing (*A–D*) or hyperpolarizing (*E–H*) direction, the membrane potential was shifted with marked over- and undershoots across the eventual steady levels.

In the records of Fig. 1 the peak amplitudes of the over- and undershoots, V_o and V_u, respectively, were measured from the later steady levels (see diagram of Fig. 2), and in Fig. 2*A* these values of V_o and V_u are plotted against the current intensities. It is seen that the magnitude of the over- and undershoots increases in an approximate proportion to the current intensity; however, the slope of this increase is significantly less for the make of depolarizing current ($2{\cdot}9$ mV/10^{-8} A) than for the make of hyperpolarizing current ($4{\cdot}4$ mV/10^{-8} A). Conversely, for the break of hyperpolarizing currents, the undershoot increases with a smaller slope ($3{\cdot}3$ mV/10^{-8} A) than for break of depolarizing currents ($4{\cdot}6$ mV/10^{-8} A).

The approximate proportionality for the I/V_o or I/V_u curve holds for current steps only within a limited range. For example, the I/V_o curve of Fig. 2*B* was obtained with a relatively wide range of current intensity (cf. Fig. 4) and shows that the slope of the curve declines as the depolarizing and hyperpolarizing currents increase in intensity.

The time course of decay of over- and undershoots

On the records of Fig. 1 the transient potential changes were measured from the steady level that obtains by about 150 msec after the onset or cessation of currents (see inset diagram of Fig. 3). When these measurements were plotted on a semilogarithmic scale as a function of time, the plotted points fell on parallel straight lines (Fig. 3*A–D*) which indicates that both the over- and undershoots decay exponentially. The time constant of this exponential decay was estimated by the reciprocal of negative slopes of the interrupted lines which in Fig. 3 were drawn visually through the plotted points. For the onset of both depolarizing and hyperpolarizing currents, the time constant was virtually the same in all curves of Fig. 3*A* and *C* (26–28 msec). On the other hand, with cessation of depolarizing currents (*B*), the time constant was slightly longer (30–32 msec), and

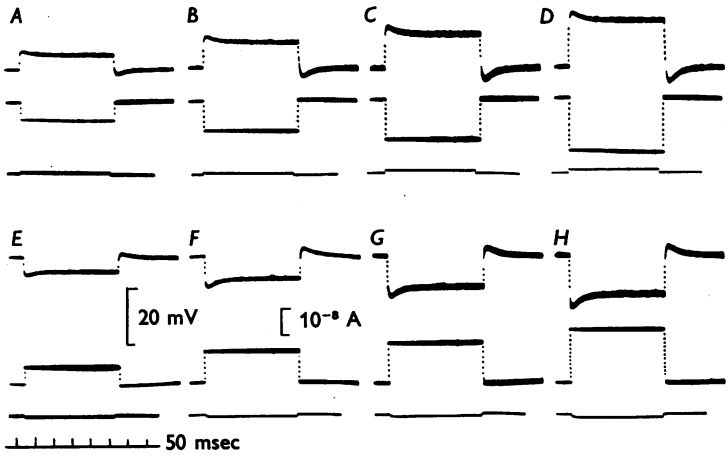

Fig. 1. Double, KCl-filled, micro-electrode. Uppermost traces, the potential changes recorded intracellularly through one barrel. Middle traces, the current steps applied through the other barrel to induce the former. Bottom traces, the extracellular records taken with the same current steps as those used intracellularly. In this as well as in the succeeding figures depolarization or positivity in the potential recording is represented by upward deflexion, while the depolarizing currents are monitored by downward deflexions.

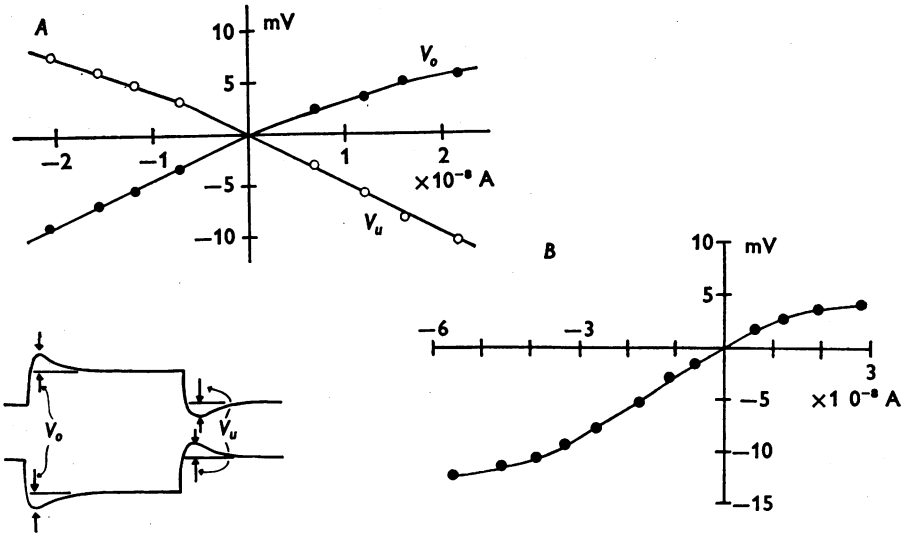

Fig. 2. *A*, plot of the peak amplitude of the over- (V_o) and undershoots (V_u) in the records of Fig. 1 as functions of the current intensities. In this as well as in Figs. 12 and 13 potential changes and currents in the hyperpolarizing direction are indicated in the negative sides of the ordinate and abscissa, respectively. The diagram below *A* shows the way to measure V_o and V_u. *B*, I/V_o curve obtained in the same motoneurone as in *A* but at a different stage of impalement. The records are partly illustrated in Fig. 4*A*, *B*.

with cessation of hyperpolarizing currents (*D*), it was still longer (36–41 msec). There were usually some discrepancies of the decay-time constants between the over- and undershoots caused by depolarizing and hyperpolarizing currents (Table 1).

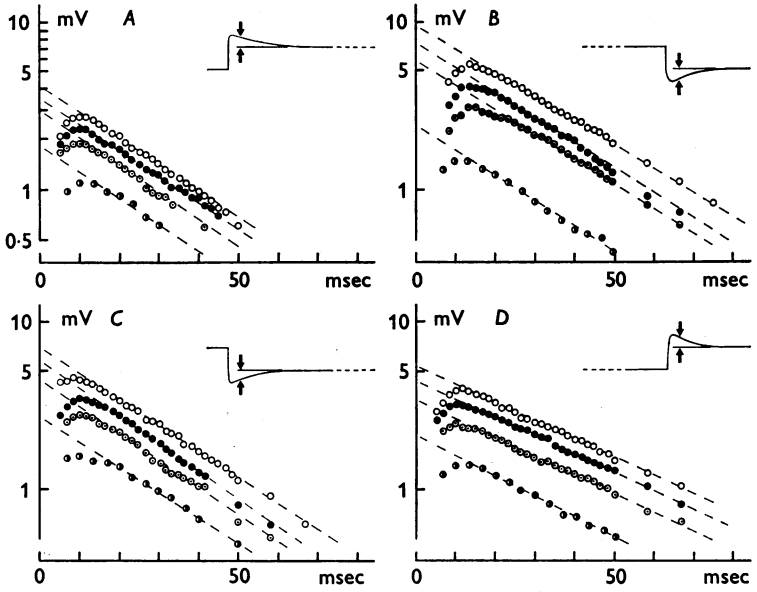

Fig. 3. Semilogarithmic plot of the decay-time course of the over- and undershoots. *A* and *B*, for make and break of depolarizing currents, respectively. *C* and *D*, for hyperpolarizing currents. Abscissae, time after the onset (*A*, *C*) or cessation (*B*, *D*) of currents. Ordinates, potential changes measured against the steady levels which are obtained in the later stage during and after current passage. Inset figures indicate the way this measurement was made. The records are illustrated in Fig. 1; ◑ for the steps in Fig. 1*A* and *E*, ⊙ for Fig. 1*B* and *F*, ● for Fig. 1*C* and *G*, ○ for Fig. 1*D* and *H*.

In Fig. 4 there are shown potential changes produced by depolarizing (*a–b*) and hyperpolarizing (*c–i*) current steps with a duration of more than 500 msec, the instant of their onset being indicated by the downward arrows in *a*. The traces in *B* were recorded simultaneously with *A*, but at five times the amplification. Close inspection of the potential changes produced by rather large current steps in *e* to *i* (Fig. 4*B*) reveals that the initial decay of the overshoot is followed by a slower decline so that even at 500 msec after the onset of current the membrane potential was still recovering. Correspondingly, when the magnitude of the overshoot is measured from the level obtaining at about 500 msec and plotted semilogarithmically, as in Fig. 4*C*, there was a deviation of the recovery curves from a simple exponential curve. The stronger the current strength, the

more they deviate. In the series of Fig. 4 large depolarizing currents were not employed, but at another trial in the same motoneurone it was seen that at more than 500 msec after the onset of a depolarizing current, even when it was as large as 5×10^{-8} A, the membrane potential was kept constant without the later slow decline that was observed with hyperpolarizing currents in Fig. 4. Large current steps were applied also in the motoneurone of Fig. 10. In spite of the relatively low gain employed there,

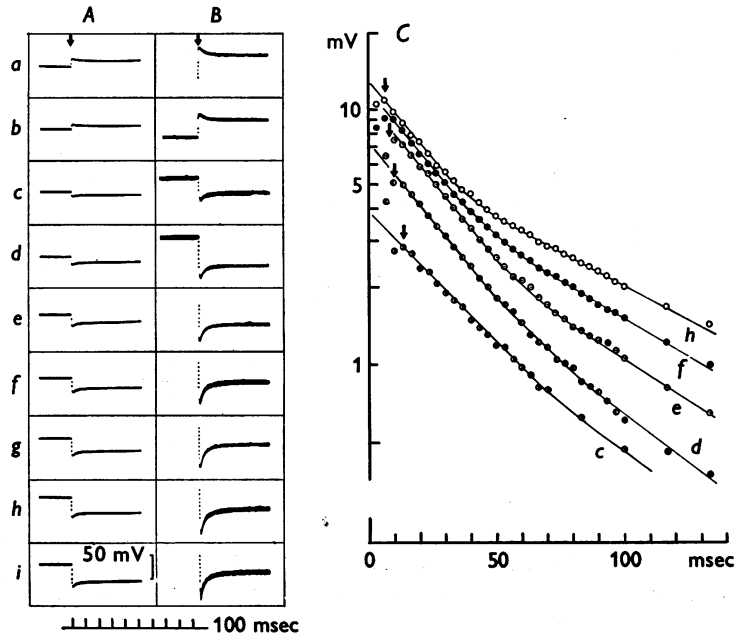

Fig. 4. Potential changes produced by prolonged current steps. *A*, *B*, records taken simultaneously at low and high (five times the former) gains, respectively. Downward arrows indicate the moment of the onset of current. *a*, *b*, depolarizing current steps. *c*–*i*, hyperpolarizing steps. Current intensities, 1·9 in *a*, 0·6 in *b*, −0·6 in *c*, −1·8 in *d*, −2·7 in *e*, −3·3 in *f*, −3·9 in *g*, −4·6 in *h*, and $-5{\cdot}6 \times 10^{-8}$ in *i*. *C*, semi-logarithmic plot of the overshoots against time after the current onset. Plot of points for the records *c*, *d*, *e*, *f* and *h* in *A* and *B*.

it may be noticed that the later slow decline was absent for large depolarizing currents (Fig. 10*Ba*, *b*) in contrast to its indication for hyperpolarizing currents (*Bg*, *h*).

Coombs, Eccles & Fatt (1955*b*) showed that, during passage of hyperpolarizing currents of 5×10^{-8} A or so through KCl-filled micro-electrode, the hyperpolarization thereby produced slowly decreased during one to two minutes after the onset of currents. This slow decline was attributed to the electrophoretic injection of chloride ions which would increase the intracellular-chloride concentration and thereby shift the membrane

potential in the depolarizing direction. Actually, records in Figs. 4 and 10 were obtained with KCl-filled micro-electrodes and therefore the above-described slow decline could be explained by an increase of the intracellular-chloride concentration. Unfortunately, no comparable tests were made with electrodes containing other anion species to substantiate this explanation.

Development of the undershoot during current steps

In Fig. 5*A–H* the duration of the current steps was increased from 1·2 to 350 msec, and correspondingly the undershoot was increased in size. In Fig. 5 *J* the potential changes produced by pulses of six different durations (*a–f*) are superposed and revealed a remarkable parallel between the decline of the overshoot and the development of the undershoot following cessation of the current.

When considering the nature of these curves, it is convenient to test how far they are superimposable. The pulse currents of various durations of

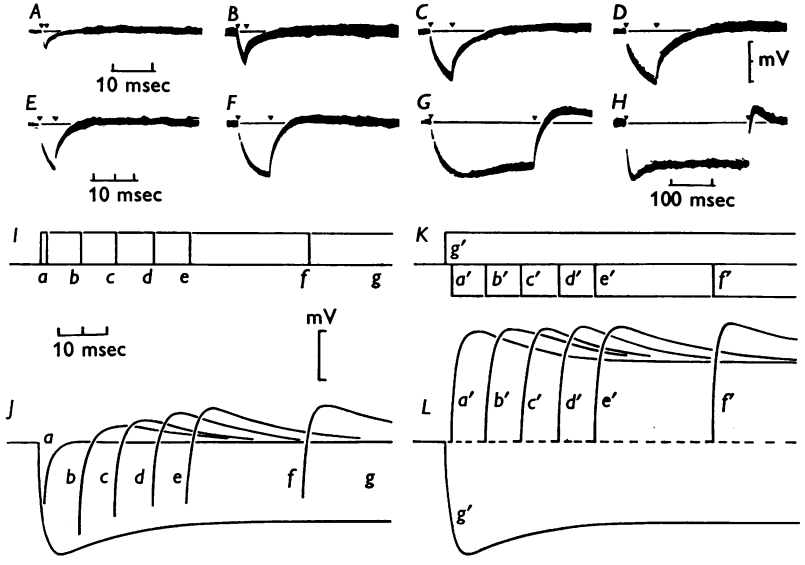

Fig. 5. Single, KCl-filled, micro-electrodes. *A–H*, hyperpolarized potential changes in a motoneurone by current steps of 3×10^{-9} A and of duration of 1 (*A*), 2 (*B*), 5 (*C*), 10 (*D*, *E*), 20 (*F*), 50 (*G*) and 350 (*H*) msec. Triangles indicate their onset and cessation. Time scale of 10 msec below *A* applies to *A–D*, and that below *E* to *E–G*, respectively. The base line is indicated by thin lines in each record. *I*, *J*, superposed tracing of the hyperpolarized potentials (*Ja–g*) produced in another motoneurone by current steps of 3×10^{-9} A and of various durations (*Ia–g*). *K*, initial (*g'*) and later (*a'–f'*) component currents of the pulses of *Ia–f*. *L*, graphical representation of the on- (*g'*) and off- (*a'–f'*) responses superposition of which yields the curves of *a–f* in *J*.

Fig. 5*I a–f* are equivalent to the superposition of two component currents, an initial indefinite current in one direction (*g'* of Fig. 5*K*) and, with various intervals, a later similar current in the opposite direction (*a'–f'* of Fig. 5*K*). Thus, if the motoneurone membrane is an ideally linear system, the potential change produced therein by the pulse current should be reproduced by a superposition of the on- and off-responses, the former being the response to the initial component current and the latter to the later component, and the on-response should, with the sign reversed, be identical to the off-response in both size and time course. In Fig. 5*L* the on-response in the motoneurone membrane (*g'*) is given by the potential curve *g* of Fig. 5*J* that was caused by current long enough to be taken as indefinite. The curves *a'–f'* of Fig. 5*L* further illustrate the deviation of the actual potential changes of Fig. 5*J a–f* from that of Fig. 5*J g*, which would represent in isolation the off-response. As would be expected from the asymmetry between the peak magnitudes of the over- and undershoots (Fig. 2*A*), a close inspection will reveal a progressive change in the off-response which occurs with increasing the pulse duration (see also next section). However, as seen in Fig. 5*L*, this change is relatively small so that the general feature of the potential changes for pulse currents may be said to be quasi-superpositional; hence it can be discriminated from those originating from the non-linear characters such as delayed rectification (see Discussion).

The initial time course of the potential changes produced by current steps

The potential changes induced by small current steps (3 and $-2{\cdot}7 \times 10^{-9}$ A) were recorded at various sweep velocities (Fig. 6) and would appear at first sight to be double exponential. After correcting for the electrode polarization given in the extracellular records of Fig. 6, the net transmembrane potential changes were reproduced graphically as shown in Fig. 7 by the onset curve of depolarization. First, the potential change during the decay of the overshoot was measured from the later steady level as V_1 (Fig. 7*A*) and was plotted semilogarithmically in Fig. 7*B* by closed circles, just in the same way as in Figs. 3 and 4*C*. The exponential curve which fits best the decay time course of the overshoot was thus determined by drawing a straight line through the plotted points of Fig. 7*B*, the initial value (E_1, see Fig. 7*A*) being given by extrapolating the abscissa to zero time. The first exponential, as it may be called, is drawn in Fig. 7*A*, *C* and *E* by interrupted lines. Secondly, the membrane potential during the initial rising phase was measured from the first exponential curve as V_2 (Fig. 7*C*) and was plotted semilogarithmically in Fig. 7*D* by closed circles, where the points fall reasonably well on a straight line except for only one point at the initial 1msec. As the best fit for V_2 the second

exponential curve with initial value of E_2 was determined. As indicated by dotted lines in Fig. 7*C* and *E*, combination of the first and second exponential curves represents the major part of the potential changes except for their very early phase. The earliest phase of the potential change was obscured by the artifact; the degree of the high frequency compensa-

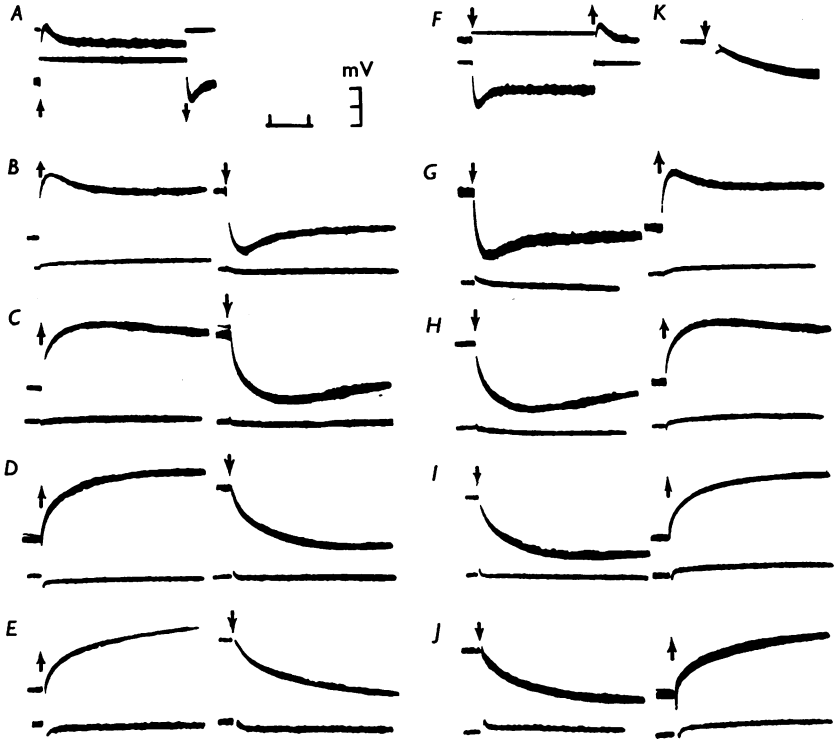

Fig. 6. Single, KCl-filled, micro-electrode. *A*, potential changes in a motoneurone caused by depolarizing current of 3×10^{-9} A. *F*, those by hyperpolarizing one of $2{\cdot}7 \times 10^{-9}$ A. *B–E* and *G–J*, showing the time courses following the onset (left column) and cessation (right column) of the depolarizing and hyperpolarizing currents, respectively, with expanded sweeps at various speeds. The time scale is equivalent to 100 msec for *A* and *F*, 40 msec for *B* and *G*, 10 msec for *C* and *H*, 4 msec for *D* and *I* and 2 msec for *E* and *J*. Upward arrows indicate the moments of onset of depolarizing currents and cessation of hyperpolarizing currents, and downward arrows mark the break of depolarizing currents and make of hyperpolarizing currents, respectively. The combined beam in *A* and *F* monitors the current steps. The lower traces in *B–E* and *G–J* are extracellular records of the electrode polarization taken in 0·15 M-KCl solution after withdrawing the electrode. *K*, further expanded record of the onset time course of the hyperpolarized potential. Time scale is 1 msec for *K*. During this recording of *K* the high frequency characteristics of the input circuit were altered from slightly under- to slightly over-compensation to demonstrate how little their adjustment influenced the potential recording except for the initial 0·5 msec.

tion significantly modified the potential curve during the initial 0·5 msec as shown in Fig. 6*K*. Nevertheless, at 1–3 msec after the current onset it was possible to follow with reasonable accuracy the potential curve which significantly deviated from the double exponential curve composed of the first and second components. The deviation was measured as V_3 (Fig. 7*E*) and its time course was roughly approximated by the third exponential curve with initial value of E_3 (Fig. 7*F*, closed circles). The time course of the potential changes following the cessation of the current was similarly analysed and their components are plotted in Fig. 7 by open circles.

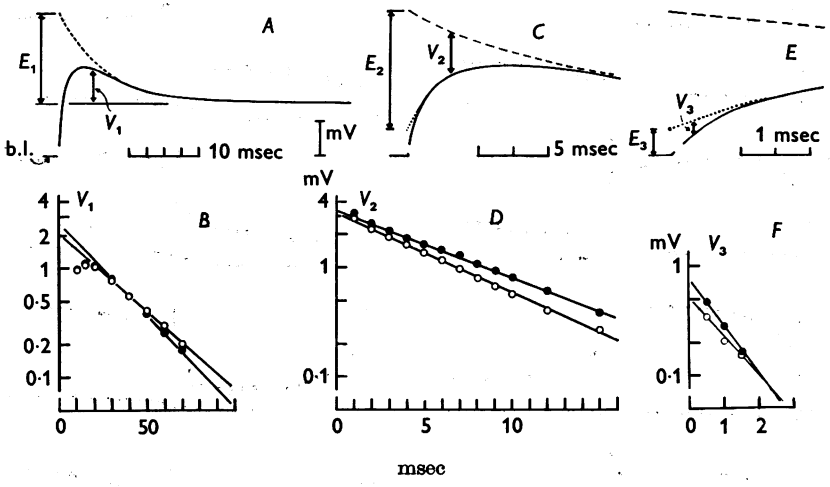

Fig. 7. *A*, *C*, *E*, transmembrane potential changes derived from the records of Fig. 6 after correcting for the electrode polarization. Explanation in text. Note that the base line (b. l. in *A*) in these tracings was drawn at an interval of $(E_1+E_2+E_3)$ from the steady level obtaining during the current passage (see eqn. 3), apart from the base line in the actual records of Fig. 6*A–E*. The latter was adjusted visually on the screen of the cathode ray oscilloscope and was found to be displaced considerably owing to the transient artifact potentials. *B*, *D*, *F*, semi-logarithmic plot of V_1, V_2 and V_3 specified in *A*, *C*, *E*, respectively (ordinates). Closed circles for the potential changes at the onset of current and open circles for those at the current cessation. Time in msec after the moment of onset or cessation of current (abscissae).

Thus the potential change V produced by current steps can be approximated by superposing three exponential curves, U_1, U_2 and U_3, with different time constants and initial values, as illustrated in Fig. 8. That is, for the make of current at the time $t = 0$,

$$V \doteq U_1+U_2+U_3$$
$$= E_1(1-e^{-t/k_1})+E_2(1-e^{-t/k_2})+E_3(1-e^{-t/k_3}), \quad (1)$$

and for the break of prolonged passage of current at $t = t_0$,

$$= E_1 e^{-(t-t_0)/k_1} + E_2 e^{-(t-t_0)/k_2} + E_3 e^{-(t-t_0)/k_3}. \quad (2)$$

Here E_1 has an opposite sign to E_2 and E_3. When the potential difference between the steady level at the later stage of current passage and the base line is measured as V_r (see diagram of Fig. 12),

$$V_r = E_1 + E_2 + E_3. \quad (3)$$

Values of the parameters involved in the equations (1)–(3) were derived from the analysis in Figs. 6–8 and are listed in Table 1*A*, together with those for another motoneurone which was investigated similarly with a single micro-electrode (*B*). U_2 component with the mean time constant of 3·9–6·0 msec may represent the membrane property in the usual sense of the capacitance-resistance model of the membrane. The actual membrane is complicated largely by superposition of the slow U_1 component which has the mean time constant of 25 msec and the initial value of reversed sign to, and 0·61–0·72 times, E_2. The other component U_3 with the mean time constant of 0·8–1·2 msec is responsible for a rather small fraction of the potential changes as indicated by the values of 0·19–0·32 for E_3/E_2. For comparison, listed in Table 1*C*, are the values for another motoneurone impaled with a double micro-electrode which allowed the application of much larger currents. In this case, the time course of V_3 could not be determined because the records were taken only with relatively slow sweep speeds. However, E_3 was calculated as the difference between V_r and $(E_1 + E_2)$ (see eqn. 3) and, relative to E_2, was found to be comparable with those in *A* and *B*. On the other hand, it is noticeable that in *C* the ratio of E_1/E_2 is about a half of that in *A* and *B*. There was a certain tendency that the ratio of E_1/E_2 was smaller with double micro-electrodes than with single ones. This may be relevant to the marked dependence of the membrane characteristics upon the membrane potential level (see below), because in general the cells were damaged more with double micro-electrodes than with single ones. It may further be seen in Table 1 that there are appreciable discrepancies between the make and break responses, in E_1, E_2 and E_3. This corresponds to the assymmetry already noticed in Fig. 2*A*, 3 and 5 between the amplitudes and time courses of the over- and undershoots. Since the sum of E_1, E_2 and E_3 is equal to V_r for either make or break of currents (eqn. 3), their changes are mutually compensatory (see Fig. 8). Hence the three components in the above-described triple exponential expression of membrane cannot be assumed to be independent of each other; but they might involve at least one non-linear factor in common.

In previous work (Frank & Fuortes, 1956; Coombs *et al.* 1959) the

TABLE 1. Data from the triple exponential analysis. Symbols as in eqns. (1)–(3)

Cell	Electrode	I (10^{-8} A)		V_r (mV)	E_1 (mV)	E_2 (mV)	E_3 (mV)	E_1/E_2	E_3/E_2	k_1 (msec)	k_2 (msec)	k_3 (msec)
A	Single	*D** 3·0	Make	1·6	−2·6	3·4	0·8	−0·76	0·24	25	6·9	1·0
			Break	—	−2·1	3·2	0·5	−0·66	0·17	30	5·8	1·3
		H† −2·7	Make	−1·3	2·6	−3·3	−0·6	−0·79	0·18	23	5·7	1·1
			Break	—	2·0	−2·8	−0·5	−0·71	0·18	23	5·5	1·3
							Mean	−0·72	0·19	25	6·0	1·2
B	Single	*D* 3·0	Make	1·9	−1·5	2·6	0·8	−0·58	0·31	26	3·3	1·2
			Break	—	−1·6	2·5	1·0	−0·64	0·40	24	5·0	0·5
		H −3·0	Make	−1·8	1·5	−2·7	−0·6	−0·56	0·22	25	3·2	0·6
			Break	—	1·6	−2·5	−0·9	−0·64	0·36	23	3·9	0·9
							Mean	−0·61	0·32	25	3·9	0·8
C	Double	*D* 22·5	Make	22·8	−9·8	25·6	7·0	−0·38	0·27	23	4·8	—
			Break	—	−4·2	20·2	6·8	−0·21	0·34	44	4·0	—
		H −21·0	Make	−20·9	7·5	−22·1	−6·3	−0·34	0·29	24	3·6	—
			Break	—	6·4	−21·1	−6·2	−0·34	0·29	30	3·6	—
							Mean	−0·32	0·30	30	4·0	—

* Depolarizing. † Hyperpolarizing. Records for *A* are shown in Fig. 6. Minus signs were attached to the figures for the hyperpolarizing currents and the potential changes in the hyperpolarizing direction.

time courses of the potential changes were studied by measuring from the level obtaining at 10–20 msec after the onset or cessation of currents, which would correspond to the summit of the over- or undershoots. From the records of Fig. 6 the potential changes were measured in the previous way as V_2' (see Fig. 9*D*) and were plotted semilogarithmically in Fig. 9*A*. From 2 to 6 msec after the onset or cessation of currents, plotted points fell on straight lines reasonably well, but with significant deviations on

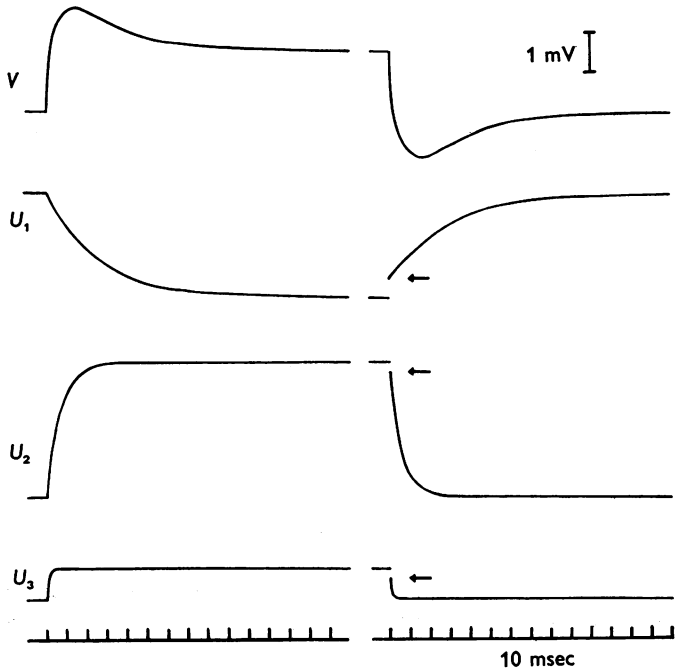

Fig. 8. Diagrams which illustrate the presumed triple exponential composition of the potential changes in the motoneurone membrane caused by current steps. V, the actual potential change. U_1, the first exponential curve. U_2, the second exponential curve. U_3, the third exponential curve. Note that the curves are interrupted before the end of the current step. Horizontal arrows indicate the starting points of the curves, U_1, U_2 and U_3, after the cessation of the current. The breaks in these curves at the end of the current pulse are due to discrepancy between the two sets of values of E_1, E_2, and E_3 calculated from the potential changes at the onset and cessation of the current (see Table 1).

both earlier and later phases of the potential rise or fall. By comparing the curves in Figs. 7*D* and 9*A*, it is obvious that correction for the first exponential curve in the former improved the exponential character of the rising or falling time course of the potential change. Rall's (1960) mathematical work indicates that, if the time course of the potential change (V) deviates from an exponential curve solely on account of the cable-like

properties of dendritic structures, plotting of $\sqrt{t}\,(dV/dt)$ will fall linearly on a semilogarithmic scale. Figure 9*B* is such a plot performed with V_2'. At 5–9 msec after the onset or cessation of currents there is a linear portion of this curve (between the upward and downward arrows). At the earlier stage the decay is slower than in the later linear phase, which Rall's (1960) calculation indicates to occur when the dendritic dominance is relatively small. However, at the very early phase of 1–2 msec (indicated by an

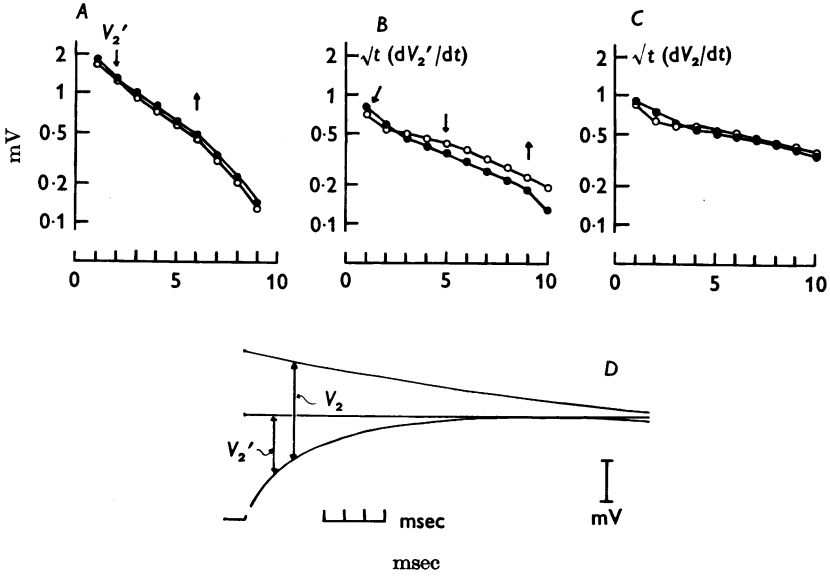

Fig. 9. *A*, *B*, *C*, semilogarithmic plots of the factors indicated for each ordinate. Abscissae represent time from onset of the applied current. Closed circles for the make of current and open circles for the break. The actual records are shown in Fig. 6*A–E*. *D*, V_2 and V_2' on the initial curve of the potential change caused by the depolarizing step.

oblique arrow), the slope of decay again becomes steeper, as already noticed by Eccles (1961), the fact being inexplicable by only the cable properties of dendritic structure. Even with plotting $\sqrt{t}\,(dV_2/dt)$, there was no appreciable improvement of linearity (Fig. 9*C*). At the present stage of investigation, combination of exponential curves such as shown in Fig. 8 appears to provide the best fit for the real potential change.

Membrane potential-dependence of the over- and undershoots

During the course of the experiments described here it was regularly noticed that, when examined with relatively small current steps, prominent over- and undershoots could be elicited only in cells with a relatively high resting potential (-60 to -80 mV). When the resting potential was

less than -50 mV there was little over- and undershoot. Hence it was thought that the electrical behaviour of the motoneurone membrane alters according to the level of the membrane potential. This suggestion is supported by the fact that in Fig. 2*B* the slope of increase of the overshoot tends to zero during a relatively large current which depolarizes the membrane. A direct proof was obtained in the following experiment.

In Fig. 10, the membrane potential was shifted over a wide range by conditioning current steps of 500 msec duration and of intentisty up to 10×10^{-8} A, while test pulses of 130 msec duration and of $12{\cdot}5 \times 10^{-9}$ A were superposed at about 200 msec after the onset of conditioning. In the non-conditioned state shown in Fig. 10*Cc*, *d* there was marked over- and undershoots except for the depolarizing on-response which was superposed by two successive spikes. In contrast, under depolarization by 50 mV (Fig. 10*Ca*, *b*) there was little over- and undershoots and the small transient changes at the onset and cessation of test pulses may be due almost entirely to the artifact which is reproduced in the extracellular records of Fig. 10*Da*, *b*. On the other hand, the over- and undershoots were maintained under conditioning hyperpolarization, as seen in Fig. 10*Ce*, *f*, *g*, *h*, though their decay time course was considerably altered (see below).

The influence which the membrane potential level has upon the over- and undershoots is also shown in records of Fig. 11, which were taken after those of Fig. 4 in the same motoneurone. In Fig. 11*A* and *B* the membrane was depolarized by 28 mV by conditioning currents (the onset is marked by downward arrow in *Aa*). At 350 msec thereafter (upward arrow) the test current steps of various intensities were superposed, and the membrane potential change during these currents were examined at a high amplification (column *B*). The decay time course of the overshoots thus obtained for test currents is plotted in Fig. 11*C* in the same way as in Fig. 4. In comparison with Fig. 4*C* it may be appreciated that the depolarizing conditioning greatly accelerates the exponential decay after the onset of the hyperpolarizing test currents. In Fig. 11*D* and *E*, on the other hand, the membrane was hyperpolarized before the application of the test currents. The semilogarithmic plot in Fig. 11*F* shows that the decay time course of the overshoot is greatly slowed down under the conditioning hyperpolarization. It was mentioned above that the decay of the overshoot under relatively large hyperpolarizing currents is composed of two phases, the initial exponential decay and the later slow phase. Inspection of Fig. 11*F* would suggest that, under conditioning by a relatively large hyperpolarizing current, the test current steps induced only the later slow phase. With increasing intensity of test currents, the initial decay of the overshoot became steeper (Fig. 11*Fe*), but still it was much slower than those observed under normal or depolarized conditions.

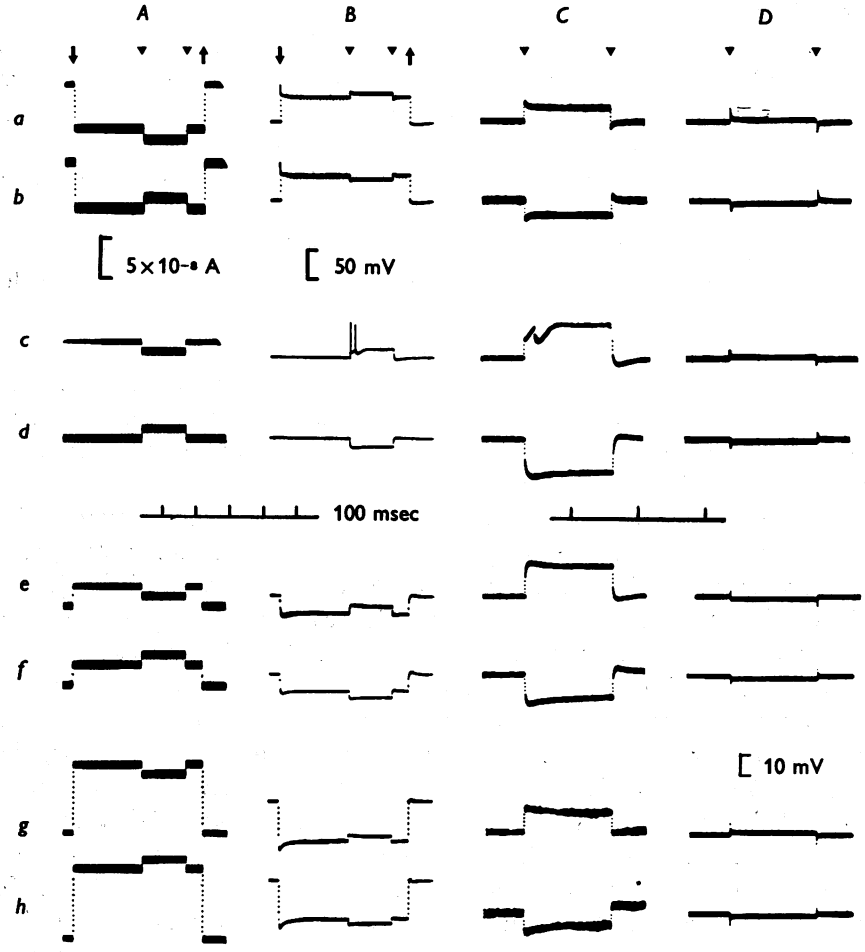

Fig. 10. Potential changes produced by superposed application of the conditioning and testing current steps. Double, KCl-filled, micro-electrode. Column *A*, current records taken from 2 kΩ inserted between the cat body and the earth. *B*, low gain d.c. records of the potential changes caused by the currents shown in *A*. *C*, illustrates the parts of *B* caused by the testing steps with a higher gain and a faster sweep speed. *D*, extracellular records taken by applying the current steps similar to those in *A*, to demonstrate the artifact involved in *C*. Rows *a*, *b*, conditioned with depolarizing currents. *c*, *d*, non-conditioned. *e*, *f*, *g*, *h*, conditioned with hyperpolarization. Upper trace of each paired records (*a*, *c*, *e*, *g*) illustrates the effect of the depolarizing test pulses. Lower trace (*b*, *d*, *f*, *h*) are for hyperpolarizing test pulses. Downward and upward arrows on the top of *A* and *B* indicate the moments of onset and cessation of current steps, respectively. Closed triangles on each column show the period of application of the test currents. Note that the voltage scale of 10 mV applies to both *C* and *D*. Two time scales of 100 msec are common in *A* and *B*, and in *C* and *D*, respectively.

Another point arising from Figs. 4 and 11 is that the summit time of the overshoot (marked by arrows in Fig. 4*C*) shortens remarkably with an increase of the test currents. According to the analyses made in Figs. 6–8, the summit time of the overshoot is determined by the characteristics of the first and second exponential curves. The shortening of the summit time is in part related to the acceleration of the decay of the first exponential curve as mentioned above, but chiefly it is caused by reduction of the time constant of the second exponential curve. The membrane potential level thus affects all the membrane properties that are concerned with the current passage, as will further be seen in the following section.

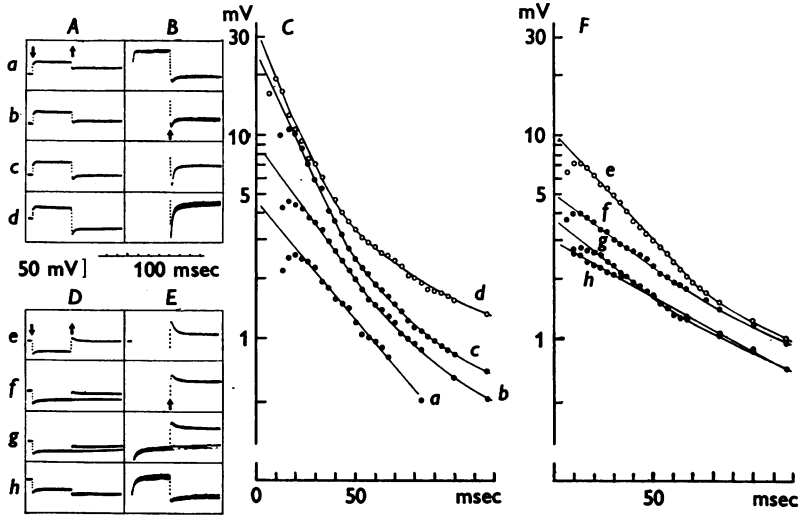

Fig. 11. Influence of the conditioning depolarization (*A*, *B*, *C*) and hyperpolarization (*D*, *E*, *F*) on the membrane responses to current steps. Specimen records of the potential changes in low (*A*, *D*) and high (*B*, *E*) gains are arranged in the same way as in Fig. 4*A*, *B*. Downward arrows in *A* and *D* indicate the moment of application of conditioning currents and upward arrows in *A* and *B* that of test currents. Intensity of the conditioning currents was $4{\cdot}8 \times 10^{-8}$ A in *A*, *B* and $-4{\cdot}3 \times 10^{-8}$ A in *D*, *E*. The strength of test steps was $-2{\cdot}0 \times 10^{-8}$ A in *a*, $-3{\cdot}0$ in *b*, $-5{\cdot}2$ in *c*, $-8{\cdot}6$ in *d*, $4{\cdot}8$ in *e*, $2{\cdot}6$ in *f*, $1{\cdot}8$ in *g* and $-2{\cdot}0$ in *h*. *C*, semilogarithmic plot of the decay time course of the overshoot in the records of *B*. Same arrangement as in Fig. 4*C*. *F*, that for the records in *E*.

The current–voltage relation of the motoneurone membrane

In previous work by Coombs *et al.* (1955*a*) the current–voltage relation was obtained by measuring the potential change under steady current flow at 2–3 sec after the current onset, while in later experiments by Coombs *et al.* (1959) pulse currents of 15–20 msec duration were employed. On account of the over- and undershoots, which have now been shown to

be a prominent feature of the motoneurone membrane, the results obtained by these two methods are expected to differ significantly.

As indicated in the inset diagram of Fig. 12, the amplitudes of the potential changes shown in the records of Fig. 1 were measured at the end of current steps as V_r and were plotted by open circles in Fig. 12*A*. This current–voltage relation (I/V_r) would correspond to those given by Coombs *et al.* (1955*a*) with steady currents, though a small discrepancy may arise from the later slow decline of hyperpolarization under relatively large currents (Fig. 4). On the other hand, closed circles in Fig. 12*A* plot the potential changes at the peak of the overshoot (V_d, see inset diagram).

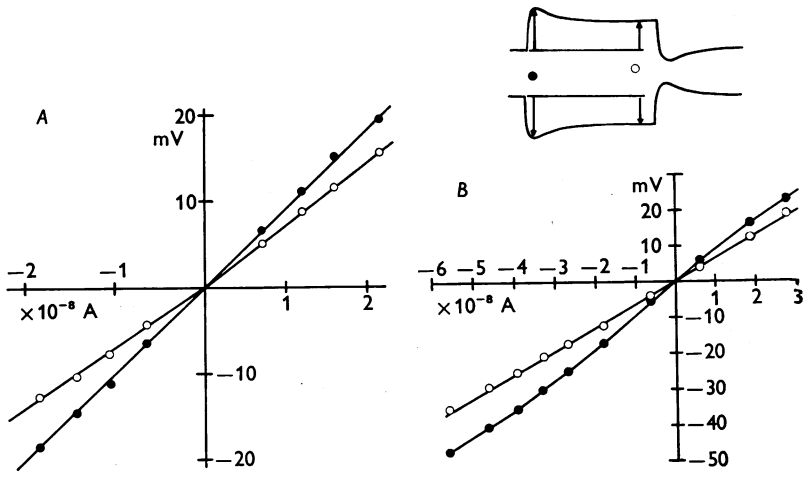

Fig. 12. Current–voltage relation of motoneurone membranes. Diagram indicates how to measure the potential changes as V_d and V_r during the current passage. *A*, taken from the records of Fig. 1. *B*, from those partly shown in Fig. 4. ● for V_d and ○ for V_r.

This current–voltage relation (I/V_d) would be equivalent to that obtained by Coombs *et al.* (1959) with relatively short pulses. Within the range of ± 20 mV in the amplitude of V_r or V_d, both the I/V_r and I/V_d curves of Fig. 12*A* are approximately linear, in agreement with the previous reports (Coombs *et al.* 1955*a*, 1959). The slope of the current–voltage relation is expressed in terms of the membrane resistance. In the I/V_r curve of Fig. 12*A* the membrane resistance is 735 kΩ for depolarizing currents and slightly smaller, 650 kΩ, for hyperpolarizing currents. Such a difference of the resistance value depending on the direction of currents was already described by Coombs *et al.* (1955*a*). In the I/V_d curve of Fig. 12 *A*, on the other hand, the membrane resistance was estimated as 875 kΩ in both depolarizing and hyperpolarizing directions. It should be emphasized

here that the membrane resistance measured by I/V_r curve is smaller by 20–30 %, or even by 40 % than the slope of I/V_d curve.

In Fig. 12*B* is plotted the I/V_r curve obtained in the series partly illustrated in Fig. 4. Over a wide range of the current strength, the plotted points fell reasonably well on a straight line, in good agreement with the results of Coombs *et al.* (1955*a*). However, owing to the non-linearity in the I/V_o curve (Fig. 2*B*), the I/V_d curve which is algebraic sum of the I/V_o and I/V_r curves deviated appreciably from a straight line under both depolarizing and hyperpolarizing currents. Another example of the I/V_r curve is illustrated in Fig. 13*A* as obtained from the series of conditioning current steps which are partly illustrated in Fig. 10; V_r was measured at 200 msec after the onset of the currents. It is remarkable in Fig. 13*A* that even the I/V_r curve is non-linear, there being considerable reduction of its slope either under depolarization or under hyperpolarization. In Fig. 13*B* the slope resistance of the membrane was determined by applying test pulses at various levels of the membrane potential that were set by passing the conditioning currents. The slope resistances thus derived as $(\Delta V_r/\Delta I)$ or $(\Delta V_d/\Delta I)$ are plotted in Fig. 13*B* as a function of the conditioning currents. As would be expected from the non-linear configuration of the I/V_r curve of Fig. 13*A*, both slope resistances are reduced by either depolarizing or hyperpolarizing conditioning. On depolarizing the membrane by more than 20 mV they fell down to about half, while they declined gradually with increasing the membrane potential, down to about half by hyperpolarization of 65 mV.

These results revealed some diversity in the current–voltage relation for different motoneuronal membranes. Among the motoneurones examined in the present experiment with double micro-electrodes, only one cell displayed a linear I/V_r curve, as shown in Fig. 12*B*, over a wide range of current intensity, while in the other six the I/V_r curve deviated considerably from a straight line as shown in Fig. 13*A*. The former cell was impaled for 3 hr with a high resting potential (−78–80 mV). The I/V_r curve of Fig. 12*B* was obtained more than 1 hr after the penetration. On the other hand, the non-linear I/V_r curves were taken at a relatively early stage of impalement, within 30 min of the penetration. It may, therefore, be suggested that the character of the I/V_r curve is transformed during the long-term impalement. Unfortunately, since there was no case where the assumed transformation of the I/V_r curve could be followed in one and the same cell, it is difficult to judge which I/V_r curve, linear or non-linear, represents the more physiological feature of the motoneurone membrane. In all motoneurones examined for the I/V_r curve, the duration of the after-hyperpolarization which follows the SD spike was uniformly short, around 100 msec (cf. Eccles, Eccles & Lundberg, 1958), indicating that these cells

all belong to the group of the fast motoneurones. Therefore, it is unlikely that the variety of the membrane property is due to different cell species of the fast and slow motoneurones. Recently, with the voltage-clamp technique, Araki & Terzuolo (1962) noticed that the voltage–current relation of the motoneurone membrane is more or less non-linear when examined over a wide range of current intensities. It was further stated by them that the non-linearity of the voltage–current relation may change its degree according to unknown conditions. This may be relevant to the above observation where a variation of the membrane property is demonstrated by current–voltage relations.

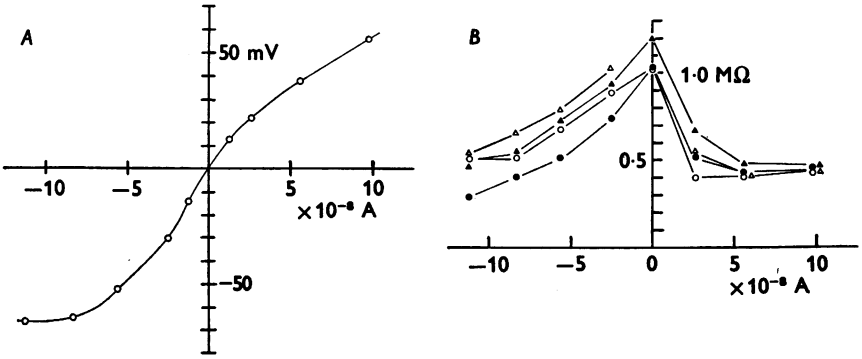

Fig. 13. *A*, an example of a non-linear I/V_r curve. The records are partly illustrated in Fig. 10. Further explanation in text. *B*, slope resistances (ordinates) at various conditioning polarizations. The abscissae represent conditioning currents similar to those in *A*. △, $\Delta V_d/\Delta I$, and ○, $\Delta V_r/\Delta I$ for depolarizing test pulses. ▲, $\Delta V_d/\Delta I$, and ●, $\Delta V_r/\Delta I$ for hyperpolarizing test pulses.

Excitability change during current steps

The excitability of the motoneurone membrane has been estimated by measuring the threshold for inducing the IS–SD spike with brief current pulses which are applied intracellularly across the motoneurone membrane. Frank & Fuortes (1956) thus found that the excitability declines slowly during application of depolarizing current steps and Coombs *et al.* (1959) further revealed the similar changes in excitability during and after passage of not only depolarizing but also hyperpolarizing currents. Araki *et al.* (1961) pointed out that these changes in the excitability closely parallel the membrane potential recorded intracellularly during and after current steps. Figure 14*A–D* shows examples of the excitability test during and after hyperpolarizing current steps, the threshold intensity of the test pulses being determined as inducing the IS–SD spikes in about half of the trials (Coombs *et al.* 1959). In Fig. 14*E* the threshold values are plotted for hyperpolarizing current steps of four different strengths. The

increase of the threshold was indicated by a downward shift of the points in accordance with the downward deflexion of the hyperpolarizing potential changes. It is obvious that the plotted points fall on curves which resemble closely the potential changes illustrated in Figs. 1, 4 and 6. The close parallelism between the membrane potential and the threshold for spike initiation is expected because the latter measures the discrepancy between the membrane potential and the certain critical level of it, provided that there is no concomitant change in the membrane impedance. It follows that the potential changes with over- and undershoots recorded intracellularly are indeed taking place across the motoneurone membrane.

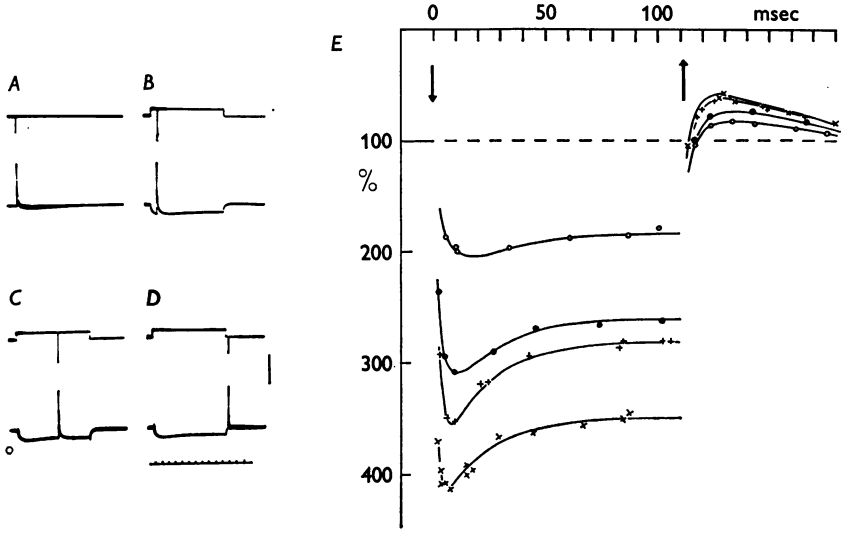

Fig. 14. *A–D*, single KCl-filled, micro-electrode. Upper traces monitor the current applied intracellularly. Lower traces represent the potential changes produced thereby. In *A*, brief depolarizing pulses (duration, 1 msec) alone were applied and induced the spikes at about half of the trials. In *B* to *D*, similar intracellular stimulation was done at various intervals from the onset of prolonged hyperpolarizing current steps. Time scale, 10 msec. The bar in *D* indicates 50 mV deflexion in the lower traces. *E*, plot of the threshold intensities for the intracellular stimulation against the time after onset of hyperpolarizing current steps of four different magnitudes. Downward and upward arrows indicate the moments of onset and cessation of currents, respectively. ○ for the records partly shown in *A–D*. Intensity of current steps; $-1{\cdot}0 \times 10^{-8}$ A for ○, $-2{\cdot}3 \times 10^{-8}$ A for ●, $-3{\cdot}0 \times 10^{-8}$ A for + and $-4{\cdot}3 \times 10^{-8}$ A for ×. The threshold is indicated in percentage relative to its values obtained without the current steps.

DISCUSSION

Marked over- and undershoots have now been shown to occur when current steps are applied across a motoneurone membrane. This particular membrane property must be contributing to the physiologically induced

potential changes, such as action potentials and post-synaptic potentials. Indeed, as noticed by Coombs, Eccles & Fatt (1955*c*), the EPSP induced monosynaptically by a volley of group Ia muscle afferent fibres (Fig. 15*A*) is followed by a small undershoot (marked by a downward arrow in Fig. 15*B*) which sums to a considerable hyperpolarization when the EPSPs are sustained by repetitive stimulation (Fig. 15*C*). When a depolarizing current was applied to the same motoneurone, there was an undershoot following its cessation (Fig. 15*D*). In their size and time course, these undershoots in *C* and *D* resemble each other, suggesting an identical origin. On the other hand, the undershoot has never been seen following an IPSP (Fig. 15*E* and *F*), but after sustained induction of IPSPs there was indication of an undershoot (marked by an arrow in Fig. 15*G*), which appears to be of the same nature as that following the EPSPs (*H*). The reason why the IPSP is less effective in producing the undershoot would be that the transmitter action for the IPSP is shorter in duration than for the EPSP (Curtis & Eccles, 1959); the shorter the duration of pulse currents, the smaller the amplitude of the undershoots (Fig. 5). With antidromic activation of motoneurones the IS spike is sometimes observed in isolation from the SD spike. It is followed by a small hyperpolarization (Fig. 15*J*), even when there is little IPSP induced through the Renshaw cell pathway (Eccles, Fatt & Koketsu, 1954). This hyperpolarization builds up to a considerable amount of undershoot when the axon is stimulated repetitively (Fig. 15*K*), as already reported by Brock, Coombs & Eccles (1953). The undershoot again resembles very much that produced by a depolarizing pulse current (Fig. 15*L*); hence presumably they are similarly generated. The after-hyperpolarization following the SD spike, on the other hand, is produced by an increased potassium conductance (Coombs *et al.* 1955*a*; Ito & Oshima, 1964*b*), and so is different from the undershoot following a depolarizing current pulse. This discrimination is obvious when sodium ions are injected into motoneurones, for the injection converts the after-hyperpolarization into a prolonged depolarization (Coombs *et al.* 1955*a*; Ito & Oshima, 1964*b*), while the undershoot after the current pulse remains practically the same as before injection (M. Ito & T. Oshima, unpublished observation). The small rebound depolarization following the after-hyperpolarization (Eccles *et al.* 1958), however, could be an undershoot of the same nature as that caused by a hyperpolarizing current steps. The excitability change of the motoneurone membrane during and after the current steps (Frank & Fuortes, 1956; Coombs *et al.* 1959) has also been shown to occur on account of the over- and undershoots of the membrane potential (Fig. 14).

Overshoots occur in squid giant axon (Hodgkin, Huxley & Katz, 1949), slow muscle fibres (Burke & Ginsborg, 1956) and in spinal ganglion cells

(toad, Ito, 1957; cat, M. Ito & T. Oshima, unpublished) due to delayed increase of the potassium conductance under flow of depolarizing currents. The mechanism for producing the overshoot in cat motoneurones, however, is apparently different from the delayed rectification for the following two reasons. First, the overshoot takes place under hyperpolarizing currents as well. Secondly, the on- and off-responses for either depolarizing or hyperpolarizing current agree with each other, at least to the extent of being superimposable (Fig. 5). If the decline of the overshoot is due to the delayed rectification, there should be a larger change in the membrane characteristics during the current flow so that the off-response would be modified in a much higher degree than actually seen (Fig. 5, Table 1). Overshoot of the hyperpolarizing potential has been seen in abdominal ganglion cells of *Aplysia* (Tauc, 1955), spinal ganglion cells (Ito, 1957; M. Ito & T. Oshima, unpublished) and in neurones of *Onchidium* (Hagiwara & Saito, 1959). This type of overshoot has been shown to be

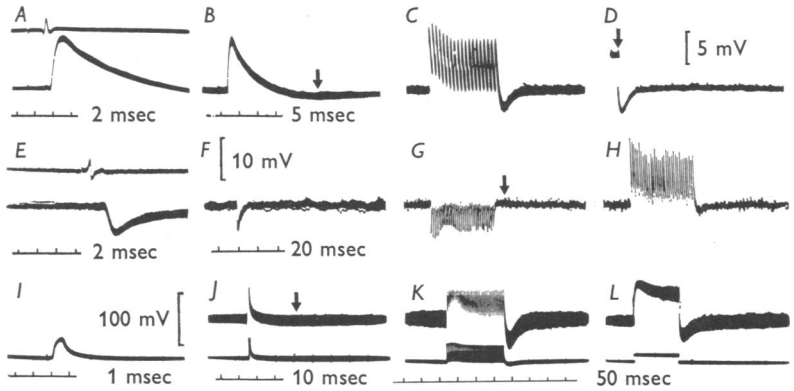

Fig. 15. *A–D*, posterior biceps-semitendinosus (PBST) motoneurone. *A*, *B*, EPSP produced monosynaptically by a synchronized volley along group Ia afferents of the PBST muscle nerve. Upper trace in *A* signals the spike potential at the entry of L7 dorsal root into the spinal cord. *C*, repetitive EPSPs similarly induced. *D*, the break response to depolarizing current steps. Downward arrow points the movement of current cessation. *E–H*, another PBST motoneurone. *E*, *F*, IPSP induced by group Ia volley from the quadriceps muscle nerve. Upper trace in *E* monitors the afferent volley similarly to that in *A*. *G*, repetitive IPSPs. *H*, repetitive EPSPs caused by stimulating the PBST muscle nerve. *I–L*, unidentified motoneurone. *I*, *J*, IS spike induced from L7 ventral root. *K*, repetitive stimulation of the L7 ventral root. Upper traces in *J* and *K* were taken simultaneously with the lower ones at a higher gain. Note that the spikes in the upper traces of *J* and *K* are truncated. *L*, potential changes caused by current steps. Lower trace in *L* monitors the applied steps. Voltage calibration of 5 mV in *D* applies to *A*, *B*, *C*, *D* and that of 10 mV in *F* to *E*, *F*, *G*, *H*. The voltage scale in *I* is 20 mV for the upper traces in *J*, *K*, *L* and 100 mV for the lower ones in *I*, *J*, *K*. Time scale of 50 msec applies to *C*, *D*, *G*, *H*, *K*, *L*. Note that in all the records the intracellular recording was done with d.c. amplification.

produced by a delayed increase of the membrane conductance and hence it has a different origin from the overshoot in spinal motoneurones of the cat.

The over- and undershoots in cat motoneurones would be accounted for by assuming that an electromotive force develops gradually during the current steps and diminishes gradually after the current ceases, as is represented by the curve U_1 in Fig. 8. Lorente de Nó (1949) described in excised nerve trunks from frogs that the electrotonic potential declines with time, much as does the overshoot in motoneurones. Actually, he assumed that this is due to a sort of nerve reaction which develops an electromotive force against the flow of extrinsic currents. Rashbass & Rushton (1949), however, maintain that the potential changes in nerve trunk are complicated by the properties of the connective-tissue sheath.

Accumulation of potassium ions in the narrow extracellular space has been assumed to have a bearing on the membrane behaviour of squid giant axon (Frankenhaeuser & Hodgkin, 1956). Such accumulation of potassium ions as this might occur around motoneurones, because the extracellular gaps are as narrow as 200 Å in width in the central nervous system (Palay, 1958; Horstmann & Meves, 1959; De Robertis & Gershenfeld, 1961). However, if potassium ions are carried out of the cell and accumulate in the extracellular cleft during flow of depolarizing currents, there will be an increase of the membrane depolarization instead of the decline actually observed. In order to explain the over- and undershoots on the basis of the accumulation of extracellular ions, it is necessary to postulate an additional factor. If the accumulated extracellular potassium be assumed to enhance the electrogenic hyperpolarizing sodium pump which appears to exist in cat motoneurones (Eccles *et al.* 1964*a*, *b*; Ito & Oshima, 1964*a*), there will be a decline of the membrane depolarization. Likwise, hyperpolarizing current flow would reduce the extracellular potassium concentration and so decrease the pump activity; there would then be a decline of the hyperpolarizing potential during the current flow. This tentative suggestion should be examined in future experiments. Since the potential changes with similar over- and undershoots were found also in the pyramidal tract cells of cat cerebral cortex (Takahashi, 1965), the problem would have a general importance in the behaviour of nerve-cell membranes.

The whole time course of the potential change during and after current steps could be approximated by combination of three exponential curves with different time constants and initial values (Fig. 8 and Table 1). The second time constant of 3·9–6·0 msec (Table 1) would correspond to the membrane time constant in the usual sense and is the main factor in determining the time course of the relatively fast membrane transient. The

time course of the fastest component, the third exponential curve, was not determined accurately because of the transient artifacts contaminating the very early phase of the potential changes at the onset and cessation of current steps. Nevertheless, the existence of this component was regularly indicated with either single or double electrodes (Table 1). Its initial values amounted to one-fifth to one-third of that for the second components (Table 1) and hence it would have a rather small influence upon the very fast transients (see below). It has already been pointed out (Fig. 9*B*, *C*) that the very early phase of the potential curve is not explicable by the cable-like properties of dendrites (Rall, 1960). However, Rall's mathematical operation was done with the basic assumption that the dendritic membrane has the same specific characteristics as those of the motoneurone soma. If a discontinuity exists between the membrane properties of these membranes, it is possible that the responses to current steps are distorted to exhibit the two quite distinct time-constant characteristics such as the second and third exponentials here described (Fig. 8). Another possibility may arise from the recent observation by Falk & Fatt (1964) on frog-muscle membrane; the initial response to current steps is composed of two fractions including time constants of 0·5 and 3·7 msec, respectively. These characteristics are attributed to the sarcoplasmic reticulum which in its effect provides a capacitance and a resistance in series, inserted in parallel with the surface membrane of muscle fibres. Resemblance of the potential curves of Fig. 8 to those in fig. 16 of Falk & Fatt (1964) would recall the abundant presence of the endoplasmic reticulum in motoneurones (Palay & Palade, 1955) which might serve as the source of distortion in the same way as assumed for the sarcoplasmic reticulum. The postulated double time constant of motoneurone membranes should be investigated further in particular connexion with the properties of the dendritic membrane and of the endoplasmic reticulum.

Relative contribution of these three components of the membrane potential change (U_1, U_2 and U_3; see Fig. 8) in producing the post-synaptic potentials can be calculated if the motoneurone membrane is assumed to be a linear system. This of course is not strictly true, but it may be allowed for as a first approximation. Thus it is assumed that the time constants and the initial values for each of the three exponential curves are invariable with respect to time, and the latter increases in proportion with the intensity of current steps (see legend to Fig. 16). An EPSP was obtained monosynaptically in the same motoneurone in which the current steps were applied, as shown in Figs. 6 and 7. First of all the post-synaptic current underlying this EPSP was worked out using either one of two sets of parameters for make or break of depolarizing currents (Table 1*A*). As illustrated in Fig. 16*F* and *J* by interrupted and

dotted lines, respectively, for the two sets of parameters, the excitatory post-synaptic current is shown to rise steeply within 0·2–0·3 msec of its onset and to fall down rapidly to some 5–10 % of the peak value, thereafter there being a slow diminution of the residual activity over about 20 msec. The general feature of these curves agrees with that previously calculated with only one time constant (Curtis & Eccles, 1959). From the post-synaptic current thus derived each component potential can be recalculated as shown in Fig. 16*G–I* and *K–M*. It is clearly seen that the second component U_2 accounts for the major part of the EPSP (Fig. 16*H*, *L*), but that the fastest component U_3 is responsible for a considerable

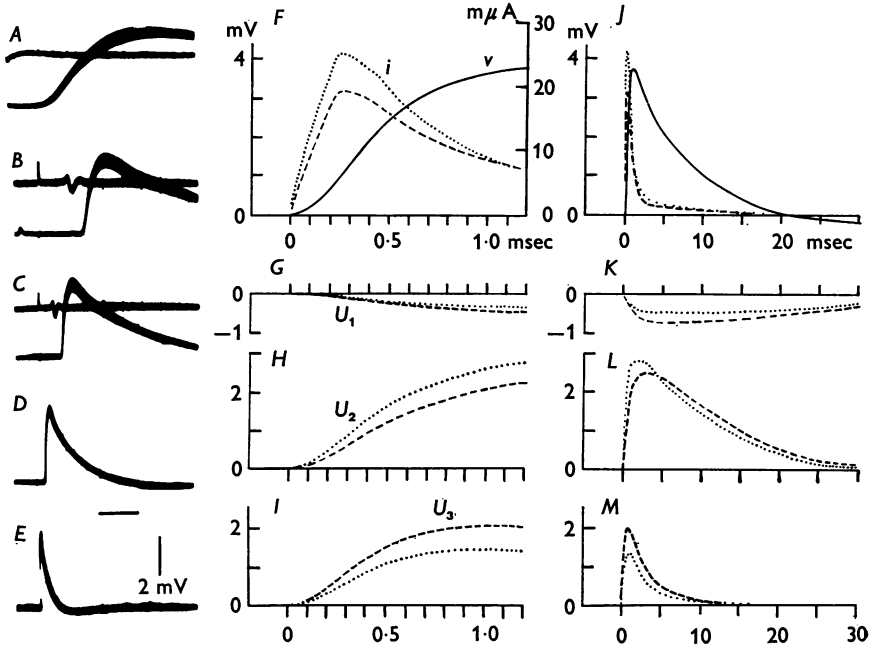

Fig. 16. *A–E*, EPSP produced by volley of group Ia muscle afferents in the motoneurone innervating the gastrocnemius-soleus muscle. Same cell as that employed for Figs. 6–9 and Table 1*A*. Time scale below *D* is equivalent to 0·4 msec for *A*, 2 msecfor *B*, 4 msec for *C*, 10 msec for *D* and 40 msec for *E*. *F*, *J*, graphical illustration of the EPSP of *A–E* (solid line, *v* in *F*) and the current which produces the former (dotted and interrupted lines, *i* in *F*). For calculating the current, the EPSP was measured at intervals of 0·1 msec in *F* and 2 msec in *J*, and for each period between these intervals the current was assumed to be rectangular. When it is further assumed that E_1, E_2 and E_3 in eqns. (1) and (2) are proportional to the current intensity (see text), the intensity of each rectangular pulse is given by eqn. (1) as the function of the potential change which it builds up at its end. The residual contribution of a pulse to the EPSP at succeeding periods is given by eqn. (2) and so can be eliminated from calculation of the effect of the succeeding pulses. *G–I*, *K–M*, components of EPSP in the triple exponential expression of the membrane characteristics. They are given in the course of the above calculation.

fraction of the early phase of the EPSP (*I*, *M*). The undershoot following the EPSP can be given by the first component U_1 that develops during the flow of the post-synaptic current (*G*, *K*). Thus even though the separation of three components is phenomenological, it is useful in attempting to understand the complex features of the membrane transients in motoneurones.

SUMMARY

1. Single and double glass micro-electrodes were inserted into lumbosacral motoneurones of cats and their electrical membrane properties were investigated with intracellular application of current steps.

2. At the onset and cessation of current steps, either depolarizing or hyperpolarizing, the membrane potential was shifted with marked over- and undershoots, respectively, which increased their amplitudes with increase in the current intensity.

3. The decay time course of the over- and undershoots was approximately exponential with a time constant of 23–44 msec. During relatively large hyperpolarizing currents the exponential decay of the membrane potential was followed by a slower decline which appeared to be absent during depolarizing currents.

4. When the current duration was increased gradually, the undershoot following the cessation of current developed in parallel with the decline of the overshoot. The effects of short pulses could be reproduced roughly by superposing the on- and off-responses to long current steps.

5. The time course of the whole potential changes during and after current steps was approximated by superposing three exponential curves, their relative initial values being $-0{\cdot}32 \sim -0{\cdot}72:1:0{\cdot}19 \sim 0{\cdot}32$ and their time constants 25 to 30, 3·9 to 6·0, and 0·8 to 1·2 msec, respectively.

6. The membrane characteristics varied according to the membrane potential. The over- and undershoots disappeared when the membrane was much depolarized, while they remained under large hyperpolarization. The depolarizing conditioning accelerated the exponential decay following the hyperpolarizing test currents, while the hyperpolarizing conditioning greatly slowed the decline of the test depolarizations.

7. The current–voltage relations were examined by measuring the peak deflexion at the overshoot (V_d) or the steady shift obtaining later during currents (V_r). Only within a limited range of currents both I/V_d and I/V_r curves are linear and an increase of currents brings about decline in the slope of I/V_d curve. In the majority of the examined cells, I/V_r curve also became non-linear and correspondingly the slope resistance declined to about half under either depolarization or hyperpolarization.

8. During and after current steps the excitability of the motoneurone

membrane was tested by measuring the threshold to induce the IS–SD spikes with brief current pulses. It followed closely the alteration of the membrane potential with the over- and undershoots.

9. Undershoots following the post-synaptic currents, IS spikes and after-hyperpolarization were explained in terms of the membrane property that causes the undershoot after current steps.

10. The factors responsible for the triple exponential characteristics of the motoneurone membrane were discussed. The slowest component was considered in conjunction with the electrogenic sodium pump, and the other two with the dendritic structure and the endoplasmic reticulum, respectively.

11. The post-synaptic current underlying an EPSP was calculated from the three time constant model of the motoneurone membrane and the relative contribution of the three components in generating the EPSP was appraised.

The authors wish to thank Prof. Sir John Eccles for his kind advice and helpful criticism during the course of this investigation and for reading this manuscript and improving the English.

REFERENCES

ARAKI, T., ITO, M. & OSCARSSON, O. (1961). Anion permeability of the synaptic and non-synaptic motoneurone membrane. *J. Physiol.* **159**, 410–435.

ARAKI, T., ITO, M. & OSHIMA, T. (1962). Potential changes produced by application of current steps in motoneurones. *Nature, Lond.*, **191**, 1104–1105.

ARAKI, T. & OTANI, T. (1955). Response of single motoneurons to direct stimulation in toad's spinal cord. *J. Neurophysiol.* **18**, 472–485.

ARAKI, T. & TERZUOLO, C. A. (1962). Membrane currents in spinal motoneurons associated with the action potential and synaptic activity. *J. Neurophysiol.* **25**, 772–789.

BROCK, L. G., COOMBS, J. S. & ECCLES, J. C. (1952). The recording of potentials from motoneurones with an intracellular electrode. *J. Physiol.* **117**, 431–460.

BROCK, L. G., COOMBS, J. S. & ECCLES, J. C. (1953). Intracellular recording from antidromically activated motoneurones. *J. Physiol.* **122**, 429–461.

BURKE, W. & GINSBORG, B. L. (1956). The electrical properties of the slow muscle fibre membrane. *J. Physiol.* **132**, 586–598.

COOMBS, J. S., CURTIS, D. R. & ECCLES, J. C. (1959). The electrical constants of the motoneurone membrane. *J. Physiol.* **145**, 505–528.

COOMBS, J. S., ECCLES, J. C. & FATT, P. (1955*a*). The electrical properties of the motoneurone membrane. *J. Physiol.* **130**, 291–325.

COOMBS, J. S., ECCLES, J. C. & FATT, P. (1955*b*). The specific ionic conductances and the ionic movement across the motoneuronal membrane that produce the inhibitory post-synaptic potential. *J. Physiol.* **130**, 326–373.

COOMBS, J. S., ECCLES, J. C. & FATT, P. (1955*c*). Excitatory synaptic action in motoneurones. *J. Physiol.* **130**, 374–395.

CURTIS, D. R. & ECCLES, J. C. (1959). The time course of excitatory and inhibitory synaptic actions. *J. Physiol.* **145**, 529–546.

ECCLES, J. C. (1961). Membrane time constants of cat motoneurones and time course of synaptic action. *Exp. Neurol.* **4**, 1–22.

ECCLES, J. C., ECCLES, R. M. & ITO, M. (1964*a*). Effects of intracellular potassium and sodium injections on the inhibitory post-synaptic potential. *Proc. Roy. Soc.* B, **160**, 181–196.

ECCLES, J. C., ECCLES, R. M. & ITO, M. (1964*b*). Effects produced on inhibitory post-synaptic potentials by the coupled injections of cations and anions into motoneurons. *Proc. Roy. Soc.* B, **160**, 197–210.

ECCLES, J. C., ECCLES, R. M. & LUNDBERG, A. (1958). The action potentials of the alpha motoneurones supplying fast and slow muscles. *J. Physiol.* **142**, 275–291.

ECCLES, J. C., FATT, P. & KOKETSU, K. (1954). Cholinergic and inhibitory synapses in a pathway from motor-axon collaterals to motoneurones. *J. Physiol.* **126**, 524–562.

FALK, G. & FATT, P. (1964). Linear electrical properties of striated muscle fibres observed with intracellular electrodes. *Proc. Roy. Soc.* B, **160**, 69–123.

FRANK, K. & FUORTES, M. G. F. (1956). Stimulation of spinal motoneurones with intracellular electrodes. *J. Physiol.* **134**, 451–470.

FRANKENHAEUSER, B. & HODGKIN, A. L. (1956). The after-effects of impulses in the giant nerve fibres of *Loligo*. *J. Physiol.* **131**, 341–376.

HAGIWARA, S. & SAITO, N. (1959). Voltage-current relations in nerve cell membrane of *onchidium verruculatum*. *J. Physiol.* **148**, 161–179.

HODGKIN, A. L., HUXLEY, A. F. & KATZ, B. (1949). Ionic currents underlying activity in the giant axon of the squid. *Arch. sci. Physiol.* **3**, 129–150.

HORSTMANN, E. & MEVES, H. (1959). Die Feinstruktur des molekularen Rindengraues und ihre physiologische Bedeutung. *Z. Zellforsch.* **49**, 569–604.

ITO, M. (1957). The electrical activity of spinal ganglion cells investigated with intracellular microelectrodes. *Jap. J. Physiol.* **7**, 297–323.

ITO, M. (1960). New electronic device for stimulation and recording potentials for a single spinal ganglion cell. In *Medical Electronics*, ed. SMYTH, C. N., pp. 84–85. London: Iliffe.

ITO, M., KOSTYUK, P. G. & OSHIMA, T. (1962). Further study on anion permeability in cat spinal motoneurones. *J. Physiol.* **164**, 150–156.

ITO, M. & OSHIMA, T. (1964*a*). The electrogenic action of cations on cat spinal motoneurons. *Proc. Roy. Soc.* B, **161**, 92–108.

ITO, M. & OSHIMA, T. (1964*b*). The extrusion of sodium from cat spinal motoneurons. *Proc. Roy. Soc.* B, **161**, 109–131.

LORENTE DE NÓ, R. (1949). A study of nerve physiology. *The studies from the Rockefeller Institute for Medical Research*, pp. 131, 132.

PALAY, S. L. (1958). The morphology of synapses in the central nervous system. *Exp. Cell Res.* **5**, 275–293.

PALAY, S. L. & PALADE, G. E. (1955). The fine structure of neurons. *J. biophys. biochem. Cytol.* **1**, 69–88.

RALL, W. (1960). Membrane potential transients and membrane time constant of motoneurons. *Exp. Neurol.* **2**, 503–532.

RASHBASS, C. & RUSHTON, W. A. H. (1949). The relation of structure to the spread of excitation in the frog's sciatic nerve. *J. Physiol.* **110**, 110–135.

DE ROBERTIS, E. D. P. & GERSCHENFELD, H. M. (1961). Submicroscopic morphology and function of glial cells. *Int. Rev. Neurobiol.* **3**, 1–65.

TAKAHASHI, K. (1965). Slow and fast groups of pyramidal tract cells and their respective membrane properties. (Prepared for publication.)

TAUC, L. (1955). Etude de l'activité élémentaire des cellules du ganglion abdominal de l'Aplysie. *J. Physiol. Paris*, **47**, 769–793.